

Document downloaded from:

<http://hdl.handle.net/10251/68176>

This paper must be cited as:

García Pérez, JV.; Carcel Carrión, JA.; Mulet Pons, A. (2012). Intensification of low-temperature drying by using ultrasound. *Drying Technology*. 30(11-12):1199-1208. doi:10.1080/07373937.2012.675533.



The final publication is available at

<https://dx.doi.org/10.1080/07373937.2012.675533>

Copyright Taylor & Francis

Additional Information



28 **Abstract**

29 Low temperature air drying involves temperatures below or close to the freezing point  
30 and aims to reduce the water content or to remove organic solvents keeping quality  
31 attributes, thus it has a great potential in food, chemical, pharmaceutical and cosmetic  
32 industries. Depending on the temperature and solvent involved, the removal is by  
33 evaporation or sublimation, but in all cases, the drying process is slow due to the low  
34 temperature used. An efficient ultrasound application at atmospheric pressure and  
35 moderate temperatures could accelerate the drying process. Thus, the main aim of this  
36 work was to test the feasibility of power ultrasound to intensify low temperature drying  
37 processes.

38 Drying kinetics of carrot, eggplant and apple cubes (side 10 mm) were carried out at  
39 atmospheric pressure, 2 m/s, -14 °C and relative humidity 7% with (acoustic power  
40 19.5 kW/m<sup>3</sup>) and without ultrasound application. At the same experimental conditions,  
41 kinetics of ethanol removal from a solid matrix were also performed. Diffusion models  
42 were used to describe drying curves and identify kinetic parameters in order to  
43 evaluate and quantify the process intensification attained by ultrasound application.

44 The effect of ultrasound application was similar for all products tested, being drying  
45 time shortened between 65-70 %. In the case of ethanol removal, the time reduction by  
46 ultrasound application was even higher achieving 120 %. Both, effective moisture  
47 diffusivity and mass transfer coefficient increased from 96 to 170 % and from 407 to  
48 428 % when ultrasound was applied, respectively. Therefore, ultrasound application  
49 should be considered a potential and effective technology to intensify low temperature  
50 drying processes, being capable to make more affordable and less energy and time-  
51 consuming these processes for all kind of industries.

52

53 Keywords: ultrasonic, atmospheric freeze drying, diffusion, mass transfer, solvent  
54 removal.

55

56 **1. Introduction**

57 The removal of solvents at low temperature is considered a common stage in food,  
58 chemical, pharmaceutical and cosmetic industries (Claussen et al., 2007; Kudra and  
59 Mujumdar, 2009; Reyes et al., 2010). Processing involves temperatures below or close  
60 to the freezing point and aims to reduce the water content or to remove organic  
61 solvents keeping quality attributes. Thus, vacuum freeze drying of pharmaceuticals  
62 (Andrieu and Vessot, 2011), atmospheric freeze drying of fish in northern Europe or  
63 drying process of dry-cured meat products (Gou et al., 2002) are some instances of low  
64 temperature drying processes. Depending on the temperature and solvent involved, the  
65 removal is by evaporation or sublimation, but in all cases, involves long drying times.  
66 As an illustration, the drying time in the processing of dry-cured ham ranges from 4  
67 month to over 2 years (Gou et al., 2002). Therefore, there exists a great opportunity for  
68 process intensification, which is a growing trend in process engineering to achieve  
69 more sustainable and affordable technologies.

70 Process intensification aims at the improvement of traditional technologies and the  
71 development of new technologies to reach higher yield, notable reduction in equipment  
72 costs, lower energy use and increase product quality and processing safety (Benali and  
73 Kudra, 2010). Traditionally, drying at low temperature has been intensified by working  
74 at vacuum conditions, which is referred to the well known conventional freeze drying,  
75 which provides high quality products and where water removal occurs mainly by  
76 sublimation and product keeps frozen. Freeze drying has high fix and operational costs  
77 (Claussen et al., 2007b) due to high energy consumption and demanding requirements  
78 of vacuum equipments and requires batch production, which makes a costly and  
79 exclusive process. Process intensification can be also addressed by coupling new  
80 technologies to atmospheric or convective freeze drying, which mainly consists of  
81 flowing air at low temperature (below freezing point) to the product being dried  
82 providing dry products with similar quality than conventional freeze dried ones (Reyes  
83 et al., 2010). In such a way, the product also keeps frozen during drying and water

84 removal occurs mainly by sublimation. The introduction of new technologies with high  
85 heating effect, such as microwave, radio-frequency and infrared radiation, should be  
86 avoided if possible due to the risk of overheating and product thawing with the  
87 subsequent reduction of the dry product quality (Riera et al., 2011). Therefore, to avoid  
88 this risk without a costly strict control of the process, non thermal strategies are mostly  
89 required for this process intensification, like the application of power ultrasound.

90 The use of power ultrasound has been recently explored for conventional hot air drying  
91 of different vegetables and fruits (Gallego-Juarez et al., 1999; Mulet et al., 2003;  
92 Garcia-Perez et al., 2011b and Riera et al., 2009). More efforts have been addressed  
93 to design and develop efficient ultrasonic devices (Gallego-Juarez et al., 2007) due to  
94 the complex application of power ultrasound in gas media. From the previous studies, it  
95 was concluded that an efficient power ultrasound application produce mechanical  
96 effects both on the gas-solid interfaces and in the material being dried. Thus,  
97 ultrasound may intensify water removal without introducing a high amount of thermal  
98 energy during drying (Riera et al., 2011). Therefore, the use of power ultrasound either  
99 to dry heat sensitive materials or to be applied in low-temperature drying processes  
100 has great potential that needs to be investigated (Garcia-Perez, 2007). Due to the  
101 ultrasound application being dependent on process and product variables, such as  
102 temperature, air velocity, acoustic power applied and product porosity, it results  
103 necessary to evaluate its feasibility when a new use is addressed.

104 Due to the lack of evidence on the efficient use of ultrasound on drying at low  
105 temperature, it is interesting to assess the feasibility of an efficient power ultrasound  
106 application to intensify this process. The drying process of vegetables products of  
107 different porosity at temperatures below freezing point will be addressed as well as the  
108 removal of other solvents from solid matrixes. Modeling was aimed at quantifying the  
109 influence of power ultrasound on mass transfer processes, although more insight will  
110 be needed in the future by considering more accurate mechanistic models.

111

## 112 2. Materials and methods

### 113 2.1. Ultrasonically assisted air drier

114 Drying experiments were carried out in a convective drier with air-recirculation,  
115 temperature and air velocity control and an ultrasonically activated drying chamber, a  
116 schematic layout of this system is shown in Fig. 1.

117 Air flow is driven by a medium pressure fan (COT-100, Soler & Palau, Spain) and  
118 measured by a van anemometer (1468, Wilh. Lambrecht GmbH, Germany). The air  
119 velocity (from 0.1 to 20 m/s) was controlled by a PID algorithm by using a digital  
120 inverter (MX2, Omron, Japan) that acts over the fan speed. In order to reach low  
121 temperatures in the air flow, a copper tube heat exchanger (area 13 m<sup>2</sup>, fin space 9  
122 mm, Frimetal, Spain) using a glycol/water solution (45 %, v/v) was installed in the air  
123 duct. A chiller (MTA, Italy) placed out of the drier provided the glycol/water solution at -  
124 22 °C and 150 L/min. The air temperature and relative humidity was measured in three  
125 points of the air duct (KDK, Galltec+mela, Germany): drying chamber inlet and heat  
126 exchanger inlet and outlet. Air temperature (from 60 to -10 °C) was also controlled by a  
127 PID algorithm acting over the electrical heating elements (maximum power 2500 W,  
128 230 V). In the temperature control system, a Pt-100 probe was used due to its shorter  
129 response time than combined air and relative humidity sensors. A compact Field Point  
130 (cFP-2220, National Instruments, USA) with RTD, analog and digital input and output  
131 modules was used to supervise and create the control loops of the air velocity and  
132 temperature.

133 In order to control the relative humidity, air flow was forced to go through 3 trays of  
134 silica gel. Each day, one tray was substituted to be re-generated (150 °C).

135 A high-power ultrasonic application system already described in previous works was  
136 assembled in the new convective drier to be used as drying chamber (Garcia-Perez et  
137 al., 2006). It mainly consists of a cylindrical radiator driven by a power ultrasonic  
138 transducer (frequency 21.9 kHz, impedance 369 Ω, power capacity 90 W). Ultrasonic  
139 signal is generated and fitted to minimize the phase between electric voltage and

140 intensity by a resonance dynamic controller (**PUSONICS**, Spain), while the power  
141 capacity is kept by acting over the power amplifier (**PUSONICS**, Spain). Finally, an  
142 impedance matching unit (impedance from 50  $\Omega$  to 500  $\Omega$  and inductance from 5 and 9  
143 mH, **PUSONICS**) is used to electrically optimize the ultrasonic application. The  
144 ultrasonic system provides an average sound pressure level in the drying chamber of  
145 155 dB. The resonance dynamic controller was connected to a PC by the RS-232  
146 interface to adequately monitor the main electric properties applied during the  
147 ultrasonic application (Power, Intensity, Voltage, Phase, Frequency and Impedance).  
148 Air flow goes through the cylindrical radiator where samples are placed. In order to  
149 determine the drying kinetics, samples are weighted at preset times by using an  
150 industrial weighing module (6000 $\pm$ 0.01 g, VM6002-W22, Mettler-Toledo, USA)  
151 connected to the compact Field Point by the RS-422 interface. A weighing sequence  
152 was programmed in the compact Field Point to make an accurate measurement: the  
153 fan was stopped and the electric slide table actuator (LEC 6, SMC, Japan) moved the  
154 samples outside the cylindrical radiator to take the weight. Thereby, the noise  
155 introduced by vibration of the cylindrical radiator in the weighing unit was avoided.  
156 An application was developed using LabVIEW2009™ programming code (National  
157 Instruments, USA) to make an overall control and monitoring of the ultrasonically  
158 intensified drying process, integrating air flow, sample and ultrasonic parameters  
159 information. The application can indistinctly run in either the PC or compact Field Point.

160

## 161 **2.2. Drying experiments**

162 Vegetal material with different internal structure was used in the drying experiments.  
163 Thus, low (carrot, var. Nantesa), medium (apple, var. Granny Smith) and high  
164 (eggplant, var. Black Enorma) porosity products (Boukouvaes et al., 2006) were  
165 purchased in local markets. For all the products, cubic samples (side 10 mm) were  
166 obtained from the flesh using a commercial slicing system (CL50E, Robot Coupe,  
167 France). Samples were wrapped using plastic and frozen by placing in a freezing room

168 at -20 °C until processing. In all cases, storage time was shorter than 72 hours. Initial  
169 moisture content was measured according to AOAC method n° 934.06 (AOAC, 1996).  
170 Air drying (AIR) experiments were carried out at  $-14\pm 1$  °C and  $2\pm 0.1$  m/s and an  
171 average relative humidity of  $7\pm 3$  %. Ultrasonically assisted air drying experiments  
172 (AIR+US) were carried out in the same experimental conditions applying an acoustic  
173 power of density  $19.5 \text{ kW/m}^3$ , which is defined as the electric power applied to the  
174 ultrasonic transducer (45 W) divided by the volume of the drying chamber (cylindrical  
175 radiator, 2.3 L). Initial mass load densities ranging between 6 (for eggplant) and  $10.5$   
176  $\text{kg/m}^3$  (for carrot) were used. Samples were weighed at preset times ranging between 1  
177 and 5 hours. Sample weight losses of 90 (eggplant), 85 (carrot) and 83 % (apple) were  
178 set to finalize the drying experiments, which were replicated, at least, three times for all  
179 conditions.

180 In order to test the ability of ultrasound to remove other solvent different to water from  
181 solid matrix, additional drying experiments were carried out. AIR dried apple samples  
182 were impregnated with ethanol (96 % v/v) at vacuum conditions (absolute pressure 0.3  
183 atm) for 60 min. Afterwards, ethanol removal experiments were carried out without  
184 (AIR) and with (AIR+US) ultrasound application at the same experimental conditions  
185 than air drying ones,  $-14\pm 1$  °C,  $1\pm 0.1$  m/s and  $19.5 \text{ kW/m}^3$ . Ethanol removal kinetics  
186 were determined by weighting samples at preset times. Experiments were replicated,  
187 at least, three times.

188

### 189 **2.3. Modeling**

190 The aim of this study being the feasibility of the use of ultrasound, thus, modeling was  
191 considered to quantify its effects by using a simplified model where water loss during  
192 drying was described by considering the diffusion theory. Eq. 1 shows the mass  
193 transfer governing equation obtained by considering a uniform temperature, constant  
194 effective diffusivity and negligible shrinkage.

195 
$$\frac{\partial W_p(x,y,z,t)}{\partial t} = D_e \left( \frac{\partial^2 W_p(x,y,z,t)}{\partial x^2} + \frac{\partial^2 W_p(x,y,z,t)}{\partial y^2} + \frac{\partial^2 W_p(x,y,z,t)}{\partial z^2} \right) \quad (\text{Eq. 1})$$

196 where  $W_p$  is the average water content (kg water/kg dry matter, dm),  $D_e$  is the average  
 197 effective diffusivity ( $\text{m}^2/\text{s}$ ),  $t$  time (s) and  $x, y, z$  represent characteristic coordinates of  
 198 cubic geometry.

199 In order to solve Eq. 1., uniform initial water content was assumed as the initial  
 200 condition. As boundary conditions, solid symmetry was considered in  $x, y$  and  $z$  mass  
 201 transfer directions. Two different approaches related to convection were taken into  
 202 consideration. As first approach, a negligible boundary layer thickness was assumed,  
 203 thus, surface water content reaches immediately the equilibrium with drying air and  
 204 mass transfer is completely controlled by internal diffusion (D Model). This boundary  
 205 condition is shown in Eq. 2 for the  $x$  mass transfer direction and the model's solution, in  
 206 terms of the average moisture content, is illustrated in Eq. 3 (Crank, 1975; Simal et al.,  
 207 1998).

208 
$$W_p(L, y, z, t > 0) = W_e \quad (\text{Eq. 2})$$

209 
$$W(t) = W_e + (W_c - W_e) \left[ \sum_{n=0}^{\infty} \frac{8}{(2n+1)^2 \pi^2} \exp\left(-\frac{D_e (2n+1)^2 \pi^2 t}{4L^2}\right) \right]^3 \quad (\text{Eq. 3})$$

210 Where  $W$  is the particle average moisture content (kg water/kg dm),  $L$  the half length of  
 211 cubic side (m) and subscripts  $c$  and  $e$  refer to critical and equilibrium states,  
 212 respectively. Sorption data at  $-10^\circ\text{C}$  reported by Claussen et al. (2007) were used to  
 213 estimate equilibrium moisture content.

214 The D Model was fitted to the experimental data in order to identify the effective  
 215 moisture diffusivity ( $D_e$ ). The objective function to be minimized was the sum of the  
 216 squared difference between experimental ( $W_{\text{exp}}$ ) and calculated ( $W_{\text{calc}}$ ) average

217 moisture content. The optimization was conducted by applying the Generalized  
218 Reduced Gradient available in Solver tool (Microsoft Excel2007™, Microsoft, USA)

219 As a second approach, boundary layer thickness was not considered negligible and  
220 mass transfer is jointly controlled by diffusion and convection (D+C Model). Eq. 4  
221 reflects this boundary condition for the x direction, representing the equality of diffusion  
222 and convection water fluxes in the interface. The D+C Model allows the quantification  
223 of both the effective diffusivity and the external mass transfer coefficient (k, kg water/m  
224 s).

$$225 \quad t > 0 \quad x = L \quad -D_e \rho_{ds} \frac{\partial W_p(L, y, z, t)}{\partial x} = k(a_w(L, y, z, t) - \varphi_{air}) \quad (\text{Eq. 4})$$

226 Where  $\rho_{ds}$  is the dry solid density (kg dm/m<sup>3</sup>), k the mass transfer coefficient (kg  
227 water/m<sup>2</sup>s), and  $\varphi_{air}$  the relative humidity of drying air. As aforementioned, the water  
228 activity in the surface of the material ( $a_w(L, y, z, t)$ ) was estimated from sorption  
229 isotherms data reported in the literature (Claussen et al., 2007).

230 The D+C Model was solved by an implicit finite difference numerical method (Garcia-  
231 Perez et al., 2011) creating a computational algorithm in Matlab® 7.9.0 (The  
232 MathWorks, Inc., USA). The program provided the local moisture distribution inside the  
233 solid and the average moisture content of the solid, both as function of the drying time,  
234 the effective moisture diffusivity ( $D_e$ ) and the mass transfer coefficient (k). As in the D  
235 model, kinetic parameters (k and  $D_e$ ) were jointly identified by fitting the model to the  
236 experimental drying kinetics. The same objective function was used than in the D  
237 model, but in this case, the SIMPLEX method (fminsearch function) available in Matlab  
238 was used for optimization.

239 Both D and D+C Models were fitted to each drying kinetic replicate and kinetic  
240 parameters averaged. The analysis of variance (ANOVA) was carried out and LSD  
241 intervals ( $p < 0.01$ ) were estimated using Statgraphics® Plus 5.1 (StatPoint, Inc., USA) to

242 evaluate the significant influence of ultrasound on  $D_e$  and  $k$  parameters. Finally, the  
243 explained variance (VAR, Eq. 5) was calculated in order to determine the goodness of  
244 the fit to the experimental data.

$$245 \quad \text{VAR} = \left[ 1 - \frac{S_{tw}^2}{S_w^2} \right] \times 100 \quad (\text{Eq. 5})$$

246 Where  $S_w^2$  and  $S_{tw}^2$  are the variance of the sample and the estimation, respectively.

247

### 248 **3. Results and discussion**

#### 249 **3.1. Drying kinetics**

250 Figure 2 shows the AIR and AIR+US drying kinetics of carrot, apple and eggplant  
251 carried out at a temperature (-14 °C) below product's freezing point. The low  
252 temperature keeps vapor pressure below the triple point and water removal mainly  
253 happens by sublimation. In such a way, this kind of experiments is commonly referred  
254 to as atmospheric or convective freeze drying.

255 Initial moisture contents were  $7.58 \pm 0.90$ ,  $6.10 \pm 0.37$  and  $14.57 \pm 0.27$  kg water/kg dry  
256 matter for carrot, apple and eggplant, respectively. The natural variability of materials  
257 being dried is showed by the drying curves in Figure 2, where it is observed that  
258 eggplant was the most heterogeneous material. Drying kinetics did not exhibit a  
259 constant rate period, which has been also reported for other products dried at low  
260 temperature (Wolff and Gibert, 1990 a and b; Kudra and Mujumdar, 2009). As a  
261 consequence, initial moisture content was considered the critical one for modeling  
262 purposes. Due to the low temperature used, drying times in AIR experiments are longer  
263 than 100 hours for apple and carrot (low and medium porosity products) and around  
264 25-30 hours for eggplant (high porosity product). The more open structure of eggplant  
265 facilitates the water vapor leaving the solid matrix by molecular diffusion, involving  
266 higher drying rates than carrot or apple. The influence of internal structure on drying

267 kinetics at temperature below freezing point has been reported in the previous literature  
268 (Claussen et al., 2007).

269 The application of power ultrasound greatly sped-up the drying kinetics. AIR+US  
270 experiments involved average reduction of drying time between 65 and 70 % for all the  
271 products. Thus in carrot experiments, to reach a moisture content of 1 kg water/kg dm,  
272 AIR experiments were extended until approximately 110 h, while AIR+US experiments  
273 only until 35 h (time reduction 68 %). In the case of eggplant, to reach a moisture  
274 content of 2 kg water/kg dm, the application of power ultrasound reduced drying time  
275 from 20 to 7 hours (time reduction 70). These results point to the fact that the ultrasonic  
276 effect was not dependent on product structure, which results opposite to the behavior  
277 observed in experiments carried out at temperatures above the product freezing point.  
278 Thus, in previous tests conducted at 40 °C, 1 m/s and applying higher acoustic power  
279 (37 against 19.5 kW/m<sup>3</sup>) than in this work, drying time was shortened by 32 % for carrot  
280 (Garcia-Perez et al., 2009) and 72 % for eggplant (Garcia-Perez et al., 2011). The fact  
281 that carrot and eggplant became different was related to porosity, thus large  
282 intercellular spaces of high porosity products make the product more prone to  
283 alternating compression and expansion cycles produced by ultrasonic waves (sponge  
284 effect) (Garcia-Perez et al., 2009). In the experiments carried out at 40 °C, shrinkage is  
285 a significant phenomenon, which keeps the product's porosity almost constant during  
286 drying due to water loss is buffered by sample volume reduction. Nevertheless, when  
287 drying at -14 °C, the shrinkage is small and regardless the initial structure, all the  
288 products are converted in high porosity matrixes. During drying at low temperature, and  
289 considering the most commonly adopted mechanistic theory of the "uniformly ice  
290 retracting front" (Claussen et al., 2007b; Wolf and Gilbert, 1990b), vapor diffusion  
291 happens in the dry outer layer, which is getting thicker as drying progresses and ice  
292 core remains in the inner part. This is the reason because of the influence of power  
293 ultrasound during drying at -14 °C was similar for carrot, apple and eggplant since all of  
294 them could be considered high porosity dry materials.

295 First attempts of using sound waves to intensify drying process at low temperature date  
296 from 70's. Moy and DiMarco (1972 and 1970) tested both the ultrasonic application at  
297 vacuum and non-vacuum freeze drying. In the case of vacuum freeze drying (Moy and  
298 DiMarco, 1972), a direct coupling between the ultrasonic transducer and the sample  
299 was adopted and the results obtained showed increments of drying rate from negligible  
300 to 6 % in beef samples. The authors concluded that the meaningful results were related  
301 to the low efficiency of the ultrasonic system used, although highlighted the potential of  
302 this technology and pointed to a better development of the ultrasonic device in order to  
303 increase efficiency. In the case of non-vacuum freeze drying, Moy and DiMarco (1970)  
304 used a stem-jet whistle working at frequencies laid between 10.8 and 12.2 kHz, which  
305 are within the human hearing range. Experiments were conducted with distilled water  
306 and coffee and tea extracts and temperatures ranging -15 and -26 °C and reported  
307 average increases of drying rate between 10 and 100 %. The main concern of this  
308 study is also related to the complex ultrasonic application in gas media, the low  
309 frequency used partially avoids the acoustic energy attenuation; this action however,  
310 may involve an intense noise that could be an obstacle to its use in industrial  
311 applications. More efforts in this field have been recently done by Bantle and Eikevik  
312 (2011) using a commercial transducer (Sonotronic, DN 20/2000, 20 kHz) and testing  
313 the influence of process variables, such as temperature and power applied. These  
314 authors showed a maximum reduction of drying time by ultrasonic application around  
315 10 % for drying green peas at -3 °C. This improvement is almost negligible compared  
316 to the results obtained in this work, and could be related to the own variability of  
317 material being dried (see Figure 2). Although the experimental reproducibility was  
318 within  $\pm 2$  %, the authors did not clarify if the improvement was significant since the  
319 statistical study to validate the results consistency is missed. In addition, as pointed out  
320 by Bantle and Eikevik (2011), the results obtained were limited by the low efficiency of  
321 the ultrasonic application system used.

322 Figure 3 shows the ethanol removal kinetics from AIR dry apple, which were carried out  
323 with the only aim of testing the ability of ultrasound to remove other solvent different  
324 than water from a solid matrix. In this case, the removal occurs by evaporation due to  
325 the freezing point of ethanol (96 % v/v) is below -14 °C. Ultrasound application also  
326 involved the increase of the drying rate, thus, the average time needed to remove  
327 completely the ethanol was reduced from 150 minutes (AIR) to 67.5 (AIR+US). This  
328 means a reduction of process time of approximately 120 %. These results open a  
329 potential application of this technology in chemical, cosmetic and pharmaceutical  
330 industry to remove organic solvents at low temperature in order to preserve quality  
331 aspects with lower processing costs than freeze drying. One of the main concerns in  
332 the use of organic solvents is the removal of traces. The cyclic and repeated vibration  
333 in the particle brought about by the ultrasonic waves could positively contribute to  
334 remove the organic solvent traces. Obviously, this hypothesis is still a challenge due to  
335 it has to be tested using more accurate detection methods than in this work, where  
336 ethanol content was monitored by weighting ( $\pm 0.01$  g) the samples at preset times.

337

### 338 **3.2. Modeling drying kinetics**

339 Modeling should concisely contribute to quantify and gain insight into the influence of  
340 ultrasound on mass transfer mechanisms involved during drying at low temperature  
341 (below freezing point). As already mentioned, the most commonly adopted mechanistic  
342 theory to describe how water removal occurs during atmospheric freeze drying is the  
343 “uniform ice retracting front” (Claussen et al., 2007b; Liapis and Bruttini, XXXX). This  
344 model considers that during drying the product is divided into two layers: a frozen inner  
345 core and a dry outer layer, being assumed that frozen core gradually and uniformly  
346 shrinking down to zero. Sublimation occurs in the ice front and water vapor moves  
347 through the dry layer to the sample surface. Therefore, mass transfer may be  
348 controlled by the internal vapor diffusion or by the external convection. According to  
349 literature (Bantle and Eikevik, 2011), water is primarily controlled by internal diffusion

350 during the atmospheric freeze drying, thus modeling may be based predominantly on  
351 diffusion. Actually, comprehensive approaches based on the “uniform ice retracting  
352 front” theory need an accurate knowledge of thermal product properties, vapor diffusion  
353 coefficients and specific porosity (Heldman and Hohner, 1974), which are temperature  
354 dependent and change during drying. Therefore, multiple assumptions and hypothesis  
355 have to be done in order to simplify the model and, sometimes, the mechanistic goal is  
356 missed and modeling approaches to empiricism. In addition, the experimental  
357 validation of the “uniform ice retracting front” models results very complicated in  
358 foodstuffs and is still a challenge. Due to modeling was not the final goal of this work,  
359 general diffusion models were used, which commonly have a good behavior for air  
360 drying at temperatures below freezing point.

361 As a first approach, drying kinetics were modeled considering a pure diffusion model (D  
362 Model) neglecting the influence on drying rate of external air flow. The effective  
363 moisture diffusivity identified from experimental kinetics, as well the explained variance  
364 attained, is included in Table 1. In AIR experiments,  $D_e$  values were  $1.1 \times 10^{-11}$ ,  $1.6 \times 10^{-11}$   
365 and  $4.8 \times 10^{-11}$   $m^2/s$  for carrot, apple and eggplant, respectively. The higher the initial  
366 product porosity, the higher the effective moisture diffusivity was found. Although,  
367 vapor diffusion occurs in the dry product layer, which is in all cases a high porosity  
368 material due to shrinkage being small, there still exists some differences in the  
369 tortuosity of water pathway due to the initial raw material properties. Due to the  
370 temperature used,  $D_e$  figures were one order of magnitude lower than the ones  
371 identified at temperatures around 30-40 °C for conventional hot air drying experiments  
372 (Garcia-Perez et al., 2009 and 2011). Furthermore, it should be remarked that the  
373 figures identified in this work would be overcome considering the “uniform ice retracting  
374 front” theory due to diffusion distance was considered as constant (L) and not variable,  
375 from 0 to L, as function of drying time or moisture content. AIR drying kinetics of carrot  
376 showed a clear diffusion behavior, being the average VAR provided by the D Model of  
377 99.3 %. This fact is also observed in Figure 4, where the fit of the diffusion model to the

378 experimental data is shown. As the initial product porosity and consequently the  
379 effective diffusivity increased, the external resistance started to be a significant  
380 phenomenon on the mass transfer control. Thus, for apple drying without ultrasound  
381 application, the drying kinetic was almost completely controlled by diffusion (VAR 98.0  
382 % from Model D), such as is observed in Figure 4. However, in the case of eggplant  
383 drying, the VAR attained with the D Model was low (93.4 %), which suggests that the  
384 influence of the external mass transfer should be considered.

385 The application of power ultrasound increased the effective diffusivity, the increase on  
386 this parameter ranged from 182 % to 244 % for carrot and apple, respectively. In all the  
387 products, the increase of the effective moisture diffusivity was significant at a  
388 significance level of 99 %. The improvement was really evident and states the high  
389 efficiency of the ultrasonic system used in this work. Bantle and Eikevik (2011) reported  
390 an increase of the effective diffusivity of up to 14.8 % in drying of green peas at -6 °C  
391 by power ultrasound application. The explained variance attained through model D in  
392 the AIR+US experiments was lower than in the AIR ones for all the products. This fact  
393 means an influence of ultrasound on mass transfer control mechanism. Thus in carrot  
394 drying, the VAR changed from 99.3 to 91.8 %, which highlights that diffusion was not  
395 the only significant mechanism controlling water removal and suggests an influence of  
396 external resistance to mass transfer when ultrasound is applied. Therefore, it seems  
397 that ultrasound had a different effectiveness over internal and external mass transfer  
398 mechanisms. In order to clarify this issue, a diffusion model including external  
399 resistance to mass transfer was considered (D+C Model).

400 The results of D+C Model are shown in Table 1, the explained variance was higher  
401 than 99.5 % in all cases, which states the significant influence of external resistance on  
402 experimental drying kinetics. The goodness of the fit achieved with the D+C Model is  
403 shown in Figure 5 for eggplant. In AIR eggplant drying and comparing with the D  
404 Model, VAR increased from 93.4 to 99.9 % (Figure 5) when considering external  
405 resistance (model D+C), being the observed increments lower for apple and carrot AIR

406 experiments where mass transfer was mainly controlled by internal diffusion. In  
407 AIR+US drying experiments, VAR ranged from 99.8 to 99.9%, being much higher than  
408 the figures attained with the D Model (from 91.8 to 92.3) (Table 1). Therefore, as  
409 already mentioned, when ultrasound was applied the importance of internal diffusion on  
410 mass transfer control was reduced. This fact is explained from the relative increase of  
411 effective moisture diffusivity and mass transfer coefficient. Average improvements from  
412 96 to 170 % were found for the mass transfer coefficient when AIR and AIR+US  
413 experiments are compared. However, the increase of the effective moisture diffusivity  
414 was laid between 407 and 428 %, which indicates that the relative importance of  
415 internal diffusion over mass transfer control was reduced when ultrasound was applied  
416 and convection plays a key role. The differences for  $D_e$  and  $k$  between AIR and  
417 AIR+US experiments were significant at a confidence level of 99 %. Maximum  
418 increases for  $D_e$  and  $k$  around 100 % have been reported in previous works carried at  
419 temperatures of 30-40 °C with different vegetables applying acoustic powers higher  
420 than in this work (García-Perez et al., 2006; Garcia-Perez et al., 2011 b and Ozuna et  
421 al., 2011). The alternating compression and expansion cycles produced by ultrasonic  
422 waves (sponge effect) should facilitate the vapor diffusion through the solid matrix. In  
423 such a way, the ultrasonic effect should not be located in the ice core if not in the dry  
424 outer layer in which vapor diffusion occurs. This is why the ultrasonic effect on the  
425 effective diffusivity was quite similar for all products (Table 1). Due to the high porosity  
426 of the dry layer, the effects brought about by compression and expansion cycles  
427 produced by ultrasonic waves are more intense than in conventionally hot air dried  
428 products where the small and water filled intercellular spaces did not allow such  
429 behaviour and diminish the ultrasonic effects (Garcia-Perez et al., 2010; Garcia-Perez  
430 et al, 2009). The high efficiency of ultrasound application over diffusion should be also  
431 linked to the greater acoustic energy absorption in high porosity products (Garcia-  
432 Perez et al., 2010). Finally, the ultrasonic effects on the external mass transfer  
433 resistance should be similar to those reported for conventional hot air drying

434 (Muralidhara et al., 1985; Gallego-Juarez et al., 1999). Pressure variations, oscillating  
435 velocities and microstreaming affect the solid-gas interfaces reducing boundary layer  
436 thickness and, therefore, improving the water transfer rate from the solid surface to the  
437 air medium.

438

#### 439 **4. Conclusions**

440 In this work, the feasibility of power ultrasound application to intensify the mass transfer  
441 rate on air drying at low temperatures (below freezing point) has been illustrated.  
442 Power ultrasound application led to a drastic reduction of drying times (around 65-70  
443 %) due to the improvement of both internal vapor diffusion and external convection.  
444 Thus, effective moisture diffusivity and mass transfer coefficient increased from 96 to  
445 170 % and from 407 and 428 %, respectively. These results showed the high efficiency  
446 of the ultrasonic application system used compared to previous literature. In addition,  
447 the ability of ultrasound to speed up the removal of ethanol from a solid matrix has  
448 been also evidenced, which opens a future application field of this technology not only  
449 in food but also in chemical, pharmaceutical and cosmetic industries to remove organic  
450 solvents preserving product quality attributes.

451 Ultrasound application should be considered a potential and effective technology to  
452 intensify low temperature drying processes, being capable to make more affordable  
453 and less energy and time-consuming these processes for all kind of industries. Future  
454 studies should be addressed to determine the influence of process parameters (air  
455 velocity and temperature, acoustic power or mass density) and optimize the ultrasonic  
456 application aiming to minimize energy consumption. Comprehensive heat and mass  
457 transfer mechanistic models considering the “uniformly ice retracting front” theory  
458 should be developed, solved, evaluated and validated. In addition, more efforts will be  
459 carried out in the design and development of new ultrasonic devices to be more  
460 efficient. Although, all these future works will have as primary goal the development of  
461 ultrasound technology for industrial applications.

462

463 **Acknowledgments**

464 The authors acknowledge the financial support to the Ministry of Economy and Finance  
465 of Spain from the Projects DPI2009-14549-C04-01 and DPI2009-14549-C04-04.

466 Moreover, the authors would like acknowledge the contribution of Ing. Ramon Peña,  
467 Cesar Ozuna and Juan V. Santacalina in the experimental work and development of  
468 the new drier device.

469

470

471 **LITERATURE**

- 472 1. AOAC. *Official methods of analysis*; Association of Official Analytical Chemist;  
473 Arlington, Virginia, USA, 1997.
- 474 2. Andrieu, J.; Vessot, S. (2011). Characterization and control of physical quality  
475 factors during freeze-drying of pharmaceutical vials. In *Modern Drying*  
476 *Technologies. Product quality and formulation (Volume 3)*. Ed. E. Tsotsas; A.S.  
477 Mujumdar. Wiley-VCH Verlag GmbH&Co. KGaA. Germany.
- 478 3. Bantle, M.; Eikevik, T.M. (2011). Parametric study of high intensity ultrasound in  
479 the atmospheric freeze drying of peas. *Drying Technology*, 29: 1230-1239.
- 480 4. Benali, M.; Kudra, T. (2010). Process intensification for drying and dewatering.  
481 *Drying Technology*, 28: 1127-1135.
- 482 5. Boukouvalas, Ch.J.; Krokida, M.K.; Maroulis, Z.B.; Marinos-Kouris, D. Density  
483 and porosity: literature data compilation for foodstuffs. *International Journal of*  
484 *Food Properties* 2006, 9, 715-746.
- 485 6. Claussen, I.C.; Strommen, I.; Hemmingsen, A.K.T.; Rustad, T. (2007).  
486 Relationship of product structure, sorption characteristics, and freezing point of  
487 atmospheric freeze-dried foods. *Drying Technology* 25: 853-865.
- 488 7. Claussen, I.C.; Ustad, T.S.; Strommen, I.; Walde, P.M. (2007b). Atmospheric  
489 freeze drying-A review. *Drying Technology* 25: 947-957.
- 490 8. Crank J. *The Mathematics of diffusion*. Oxford (2nd ed.), UK, Clarendon Press.  
491 **1975.**
- 492 9. Gallego-Juárez, J.S.; Rodriguez-Corral, G.; Galvez-Moraleda, J.C.; Yang T.S.  
493 (1999). A new high intensity ultrasonic technology for food dehydration. *Drying*  
494 *Technology* 17: 597-608.
- 495 10. Gallego-Juarez, J.A.; Riera, E.; de la Fuente-Blanco, S.; Rodriguez-Corral, G.;  
496 Acosta-Aparicio, V.M., Blanco, A. (2007). Application of high power ultrasound

- 497 for dehydration of vegetables: Processes and devices. *Drying Technology* 25:  
498 1893-1901.
- 499 11. Garcia-Perez, J.V. (2007). Contribución al estudio de la aplicación de  
500 ultrasonidos de potencia en el secado convectivo de alimentos. PhD Thesis.  
501 Universitat Politècnica de Valencia.
- 502 12. García-Pérez J.V., Cárcel J.A., De la Fuente S. and Riera E., Ultrasonic drying  
503 of foodstuff in a fluidized bed. Parametric study. *Ultrasonics* 44: e539-e543  
504 (2006).
- 505 13. García-Pérez, J.V.; Ozuna, C.; Ortuño, C.; Cárcel, J.A.; Mulet, A. Modeling  
506 ultrasonically assisted convective drying of eggplant. *Drying Technology* 2011a  
507 29, 1499-1509.
- 508 14. Garcia-Perez, J.V., Ortuño, C., Puig, A., Carcel, J.A., Perez-Munuera, I. (2011).  
509 Enhancement of water transport and microstructural changes induced by high  
510 intensity ultrasound application on orange peel drying. *Food and Bioprocess*  
511 *Technology*, in press.
- 512 15. Garcia-Perez, J.V., Carcel, J.A., Riera, E., Mulet, A. 2009. Influence of the  
513 applied acoustic energy on the drying of carrots and lemon peel. *Drying*  
514 *Technology* 27, 281-287.
- 515 16. Gou, P.; Comaposada, J.; Arnau, J. (2002), Meat pH and meat fibre direction  
516 effects on moisture diffusivity in salted ham muscles dried at 5 °C. *Meat*  
517 *Science*, 61: 25-31.
- 518 17. Heldman, D.R.; Hohner, G.A. (1974). An analysis of atmospheric freeze drying.  
519 *Journal of Food Science* 39: 147-155.
- 520 18. Kudra, T.; Mujumdar, A.S. (2009). Atmospheric freeze drying. In *Advanced*  
521 *Drying Technologies*. 2<sup>nd</sup> Ed. CRC Press.
- 522 19. Moy, J.H.; DiMarco, G.R. (1972). Freeze-drying with ultrasound. *Transactions*  
523 *of the ASAE*, 373-376.

- 524 20. Moy, J.H.; DiMarco, G.R. (1970). Exploring airborne sound in a nonvacuum  
525 freeze drying process. *Journal of Food Science*, 35: 811-817.
- 526 21. Mulet., A., Cárcel, J.A., Sanjuán, N., Bon, J. (2003b). New food drying  
527 technologies-Use of ultrasound. *Food Science and Technology International* 9:  
528 215-221.
- 529 22. . Muralidhara, H.S., Ensminger, D.; Putnam, A. (1985). Acoustic dewatering and  
530 drying (low and high frequency). State of the art review. *Drying Technology* 3:  
531 529-566.
- 532 23. Reyes, A.; Vega, R.V., Bruna, R.D. (2010). Effect of operating conditions in  
533 atmospheric freeze drying of carrot particles in a Pulsed Fluidized bed. *Drying*  
534 *Technology*, 28: 1185-1192.
- 535 24. Riera, E., García-Pérez, J.V., Acosta, V.M., Carcel, J.A., Gallego-Juárez, J.A.  
536 (2011). A computational study of ultrasound-assisted drying of food materials.  
537 In *Multiphysics Simulation of Emerging Food Processing Technologies*. Ed. Kai  
538 Knoerzer, Pablo Juliano, Peter Roupas and Cornelis Versteeg, IFT Press, 265-  
539 302.
- 540 25. Simal, S.; Rosello, C.; Mulet, A. (1998). Modelling of air drying in regular  
541 shaped bodies. *Trends in Chemical Engineering*, 4(4), 171-180.
- 542 26. Wolff, E.; Gilbert, H. (1990a). Atmospheric freeze drying. Part 1: Design,  
543 experimental investigations and energy-saving advantages. *Drying Technology*,  
544 8: 385-404.
- 545 27. Wolff, E.; Gilbert, H. (1990b). Atmospheric freeze drying. Part 2: Modelling  
546 drying kinetics using adsorption isotherms. *Drying Technology*, 8: 405-428.  
547

548 **FIGURE CAPTIONS**

549

550 Figure 1. Diagram of the ultrasonically assisted convective drier. 1. Fan, 2.  
551 Anemometer, 3. Temperature and relative humidity sensor, 4. 3-Way valve, 5.  
552 Ultrasonic transducer, 6. Vibrating cylinder, 7. Sample load device, 8. Retracting pipe,  
553 9. Slide actuator, 10. Weighing module, 11. Heat exchanger, 12. Heating elements, 13.  
554 Desiccant tray chamber. 14. Pt-100.

555

556 Figure 2. Experimental drying kinetics of carrot, apple and eggplant. AIR: Conventional  
557 drying experiments (-14 °C, 1 m/s) and AIR+US: Ultrasonically assisted drying  
558 experiments (-14 °C, 1 m/s, 19.5 kW/m<sup>3</sup>).

559

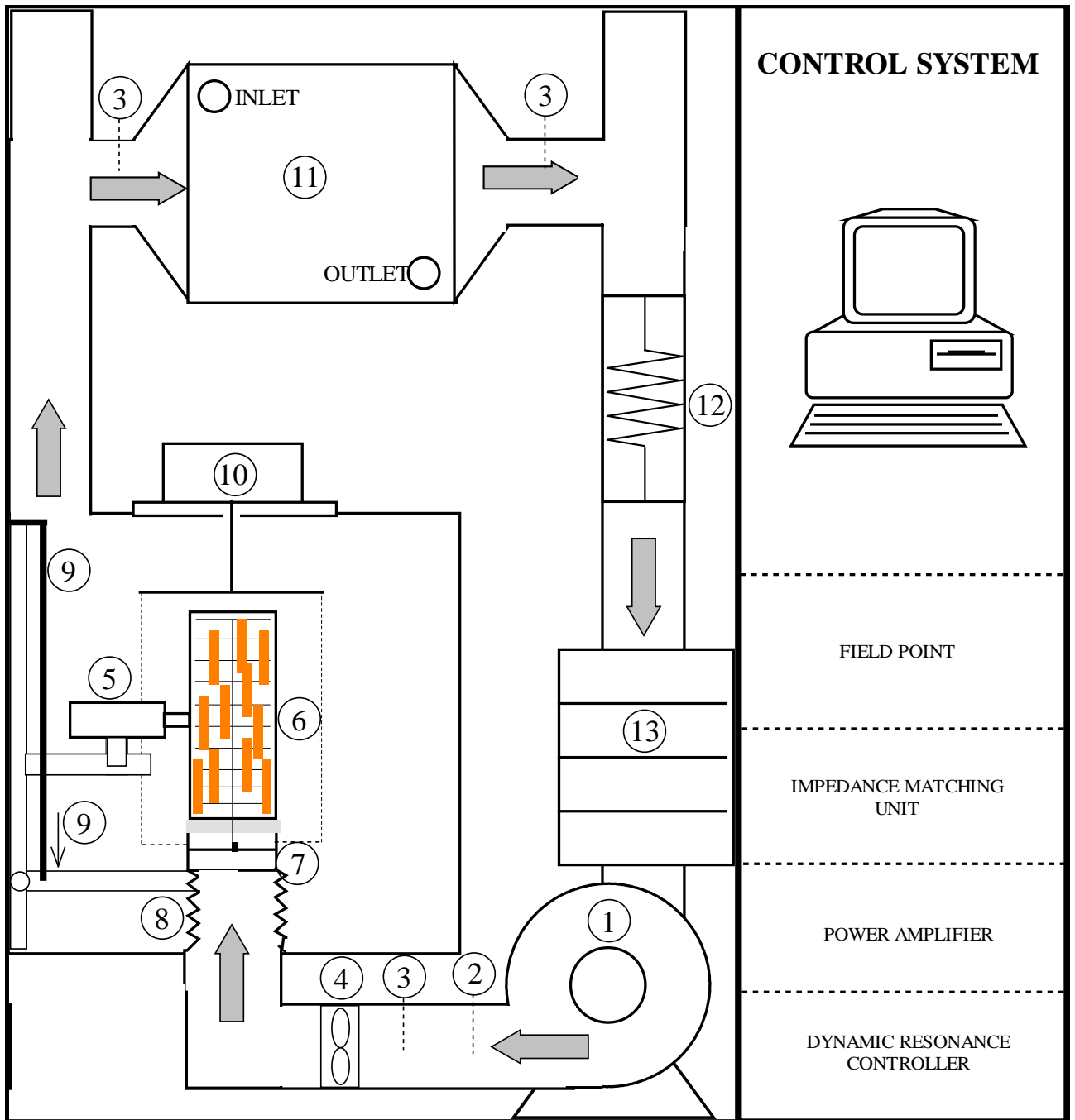
560 Figure 3. Kinetics of ethanol removal from AIR dried apple. AIR: Conventional drying  
561 experiments (-14 °C, 1 m/s) and AIR+US: Ultrasonically assisted drying experiments (-  
562 14 °C, 1 m/s, 19.5 kW/m<sup>3</sup>).

563

564 Figure 4. Fit of the D model to the drying kinetics of carrot and apple. AIR:  
565 Conventional drying experiments (-14 °C, 1 m/s) and AIR+US: Ultrasonically assisted  
566 drying experiments (-14 °C, 1 m/s, 19.5 kW/m<sup>3</sup>). In each plot, only one replicate is  
567 included.

568

569 Figure 5. Fit of the D+C model to the drying kinetics of eggplant. AIR: Conventional  
570 drying experiments (-14 °C, 1 m/s) and AIR+US: Ultrasonically assisted drying  
571 experiments (-14 °C, 1 m/s, 19.5 kW/m<sup>3</sup>). In each plot, all the replicates are included  
572 with the simulation.



573

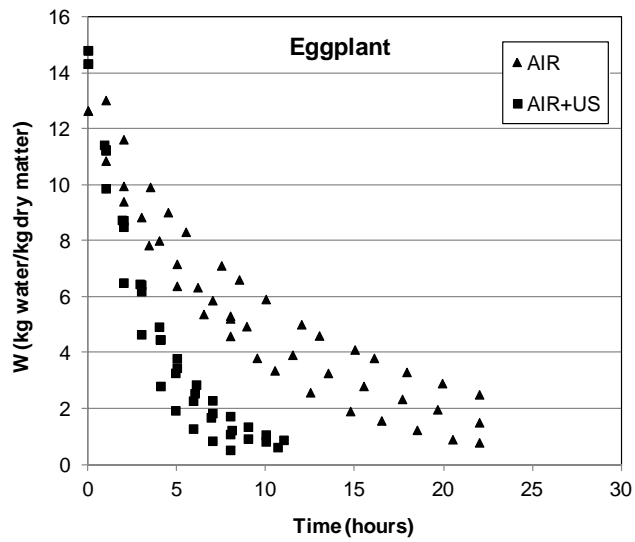
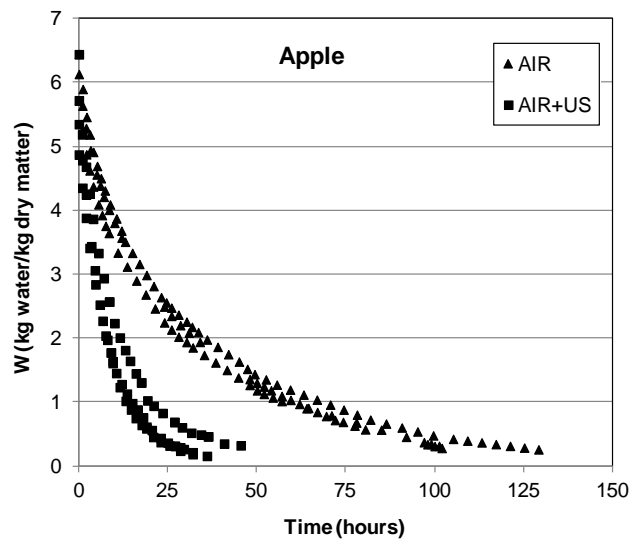
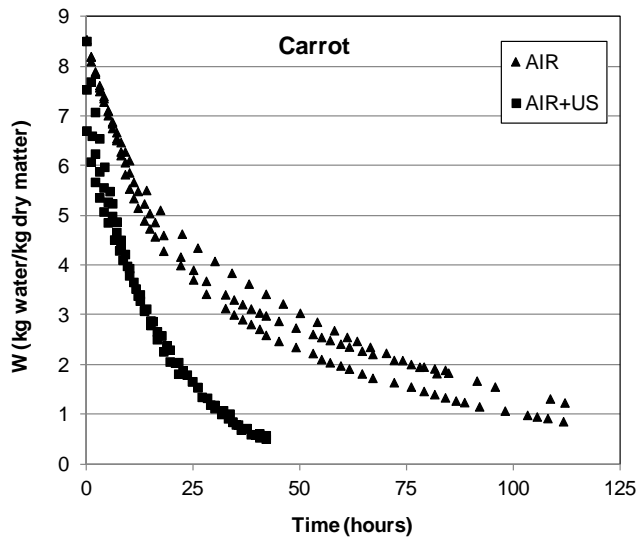
574

575

576

577

**Figure 1**

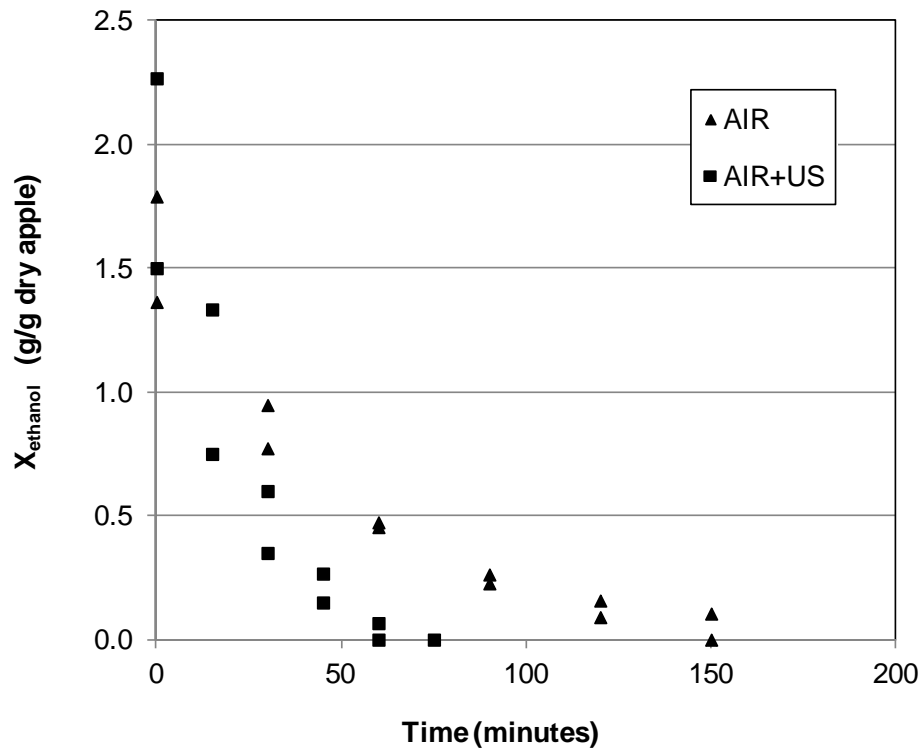


578

579

580

**Figure 2**



581

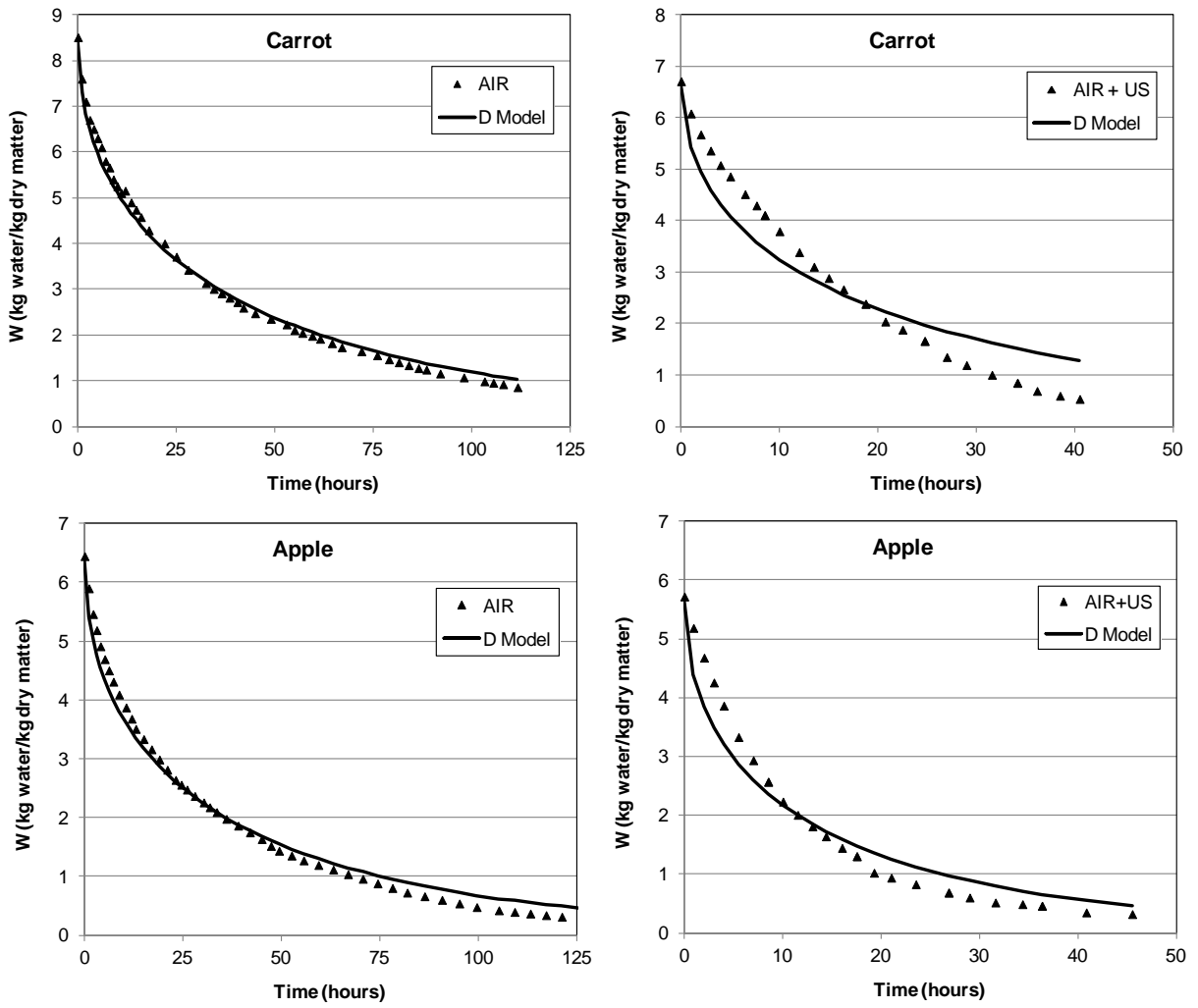
582

583

584

Figure 3

585



586

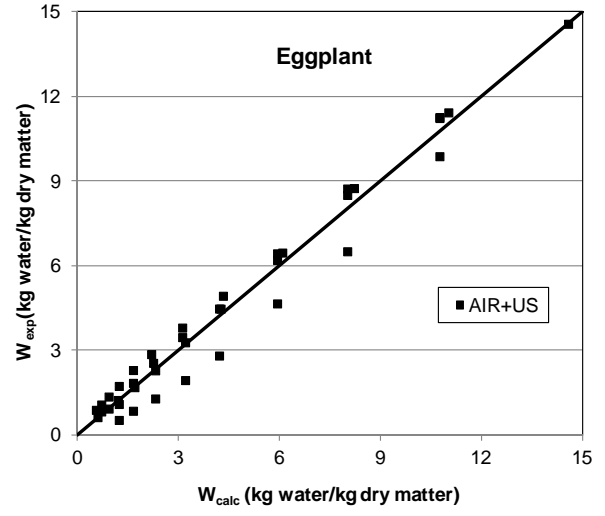
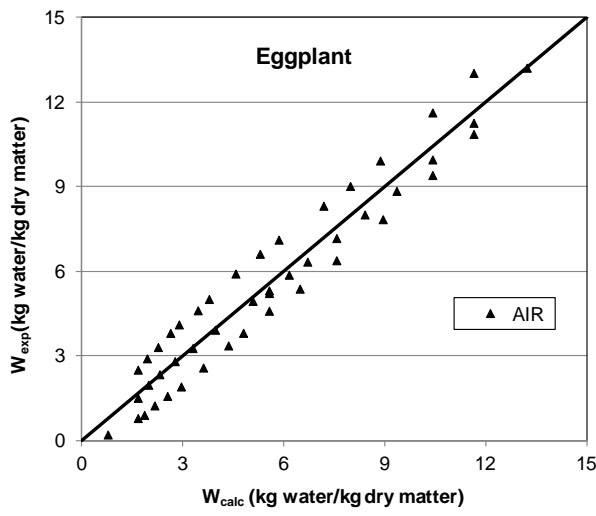
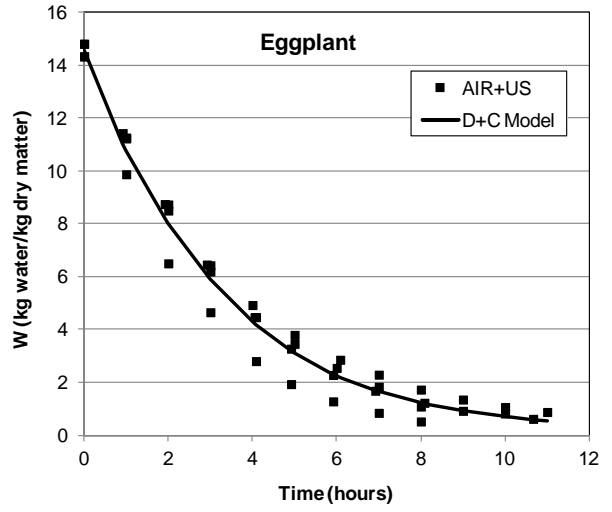
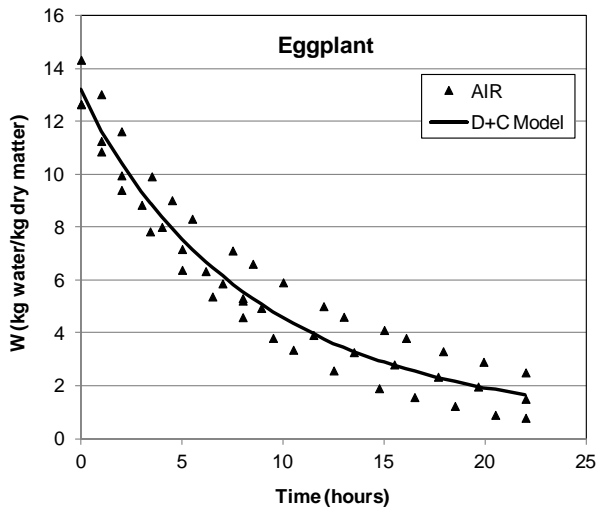
587

588

589

590

Figure 4



591

592

593

594

**Figure 5**

595  
596

Table 1. Results of drying kinetics modeling. Average values and standard deviation of kinetic parameters identified from D and D+C Models. Increment shows (in percentage) the increase of a kinetic parameter by the application of ultrasound.

		<b>D MODEL</b>		<b>D+C MODEL</b>		
		<b>D<sub>e</sub> (10<sup>-11</sup> m<sup>2</sup>/s)</b>	<b>VAR (%)</b>	<b>D<sub>e</sub> (10<sup>-11</sup> m<sup>2</sup>/s)</b>	<b>k (10<sup>-5</sup> kg water/m<sup>2</sup> s)</b>	<b>VAR (%)</b>
<b>Carrot</b>	<b>AIR</b>	1.1±0.1	99.3	0.8±0.1	3.3±1.5	99.6
	<b>AIR+US</b>	3.1±0.3	91.8	4.2±0.4	8.3±2.3	99.8
	<b>Increment (%)</b>	182		425	152	
<b>Apple</b>	<b>AIR</b>	1.6±0.4	98.0	1.4±0.7	4.8±0.2	99.5
	<b>AIR+US</b>	5.5±1.1	93.3	7.4±2.1	9.4±0.9	99.9
	<b>Increment (%)</b>	244		428	96	
<b>Eggplant</b>	<b>AIR</b>	4.8±1.3	93.4	4.4±1.7	23.7±4.3	99.9
	<b>AIR+US</b>	15.8±3.3	92.3	22.3±4.7	64.1±10.4	99.9
	<b>Increment (%)</b>	229		407	170	

597  
598